# Chemiluminescent Reactions of Lucigenin. 2. Reactions of Lucigenin with Hydroxide Ion and Other Nucleophiles

**Richard Maskiewicz, Dotsevi Sogah, and Thomas C. Bruice***

*Contribution from the Department of Chemistry, University of California at Santa Barbara, Santa Barbara, California 93106.* *Received December 26, 1978*

**Abstract:** The reactions undergone by lucigenin (*N,N'*-dimethyl-9,9'-biacridinium dication, **1**) in alkaline solutions in the presence of molecular oxygen are very complex, yielding as products *N*-methylacridone (**2**), *N,N'*-dimethyl-9,9'-biacrylidine (**3**), *N,N'*-dimethylacrylidene oxide (**4**), *N,N'*-dimethyl-9,9'-dihydroxybiacridan (**5**), *N*-methylacridanol (**6**), and *N*-methylacridan (**7**). A very minor reaction (quantum yield ($\Phi_{CL}$) = $1 \times 10^{-4}$) provides excited *N*-methylacridone (**2***). Under the pseudo-first-order conditions of the present investigation ([**1**] = $1.75 \times 10^{-5}$ M, [$O_2$] = $1.5 \times 10^{-4}$ M, and at constant pHs) the minor chemiluminescent (CL) reaction and the major and non-CL reactions comprise competing parallel first-order paths for the disappearance of **1**. The pseudo-first-order rate constants for disappearance of **1** must then (and do) equal the pseudo-first-order rate constants for the decay of intensity of photon emission. The rate law for the consumption of **1** ($-d[\mathbf{1}]/dt = \{k_1[HO^-] + k_2[HO^-]^2\}[\mathbf{1}]$) establishes that the critical transition states for the reactions leading to **2–7** are composed of one molecule of **1** and one or two $HO^-$ ions (dependent upon pH). The rate law for the formation of **2*** via the CL reactions has been obtained from the concentration dependencies of the quantum yields ($\Phi_{CL}$) and the rate law for disappearance of **1**. The critical transition states for the CL reactions are composed of two molecules of **1** and one or two $HO^-$ ions (dependent upon pH) [i.e., $d[\mathbf{2}^*]/dt = \{k[HO^-] + k[HO^-]^2\}[\mathbf{1}]^2$]. Addition of one $HO^-$ to **1** is reversible ($pK_a$ = 12.43) while addition of a second $HO^-$ species is only partially reversible (i.e., $\mathbf{1} + HO^- \rightleftarrows \mathbf{1}(OH)$; $\mathbf{1}(OH) + HO^- \rightarrow \mathbf{1}(OH)_2$). The major non-CL reactions and the minor CL reactions arise from the partitioning of **1**(OH) and **1**$(OH)_2$. Thus, for the CL reactions $d[\mathbf{2}^*]/dt = k_x[\mathbf{1}][\mathbf{1}(OH)] + k_y[\mathbf{1}][\mathbf{1}(OH)_2]$ while for the non-CL reaction $d[\mathbf{1}]/dt = k_1[\mathbf{1}(OH)] + k_2[\mathbf{1}(OH)_2]$. That intermediate **1**(OH) reacts with **1** to provide **2*** is supported by the finding of a lag phase in the formation of **2*** which can be shown (by way of the concentration dependence for the exponential increase in the intensity of photon emission) to be first order in [**1**] and [$HO^-$]. Nucleophiles of sufficient basicity ($CF_3CH_2O^-$, $CN^-$, $CH_3CH_2NH_2$) may substitute for $HO^-$ to provide chemiluminescence. In the reactions of **1** with $HO^-$ and $CF_3CH_2O^-$ the lag phase in photon emission is accompanied by a very similar lag phase in ESR signal intensity. Both the intensity of the ESR signal and the value of the integrated photon emission increase and become constant at comparable times. The mechanisms for the CL reactions are suggested to involve $1e^-$ transfer from the nucleophilic adducts of **1** (i.e., when nucleophile = $HO^-$ the adducts are **1**(OH) and **1**$(OH)_2$) to **1**, converting the latter to **1**· which then reacts with molecular oxygen to provide the dioxetane (**1**(OO)). Thermal cleavage of **1**(OO) provides **2** + **2***. That $1e^-$ transfer to **1** from dihydroacridine structures (as **1**(OH) and **1**$(OH_2)$) provides chemiluminescence in the presence of molecular oxygen has been demonstrated by the intense and $O_2$-dependent chemiluminescence seen when **1** reacts with the dihydrobiacridines **3** and **4**.

## Introduction

In the previous paper the CL reaction of lucigenin (**1**) with hydrogen peroxide[1] was examined. The present study concerns the mechanisms of chemiluminescence accompanying the reaction of **1** with various nucleophiles under aerobic conditions.[2-6] Our primary interest has been the CL reaction of **1** with hydroxide ion. These CL reactions have been of continuing concern for some years. Previous kinetic approaches to mechanisms have been futile since the determined concentration dependencies of rate constants by themselves only provide information about the major and non-light-producing reaction(s)—i.e., A → B of eq 1.

$$\mathrm{A} \xrightarrow{k_1} \mathrm{B} \qquad \text{where } k_1 \gg k_2 \qquad (1)$$
$$\mathrm{A} \xrightarrow{k_2} \{\mathrm{C}^{\ddagger}\} \longrightarrow \mathrm{C} + h\nu$$

However, it is possible to define the composition of the rate-determining transition states for two competing parallel pseudo-first-order reactions when one reaction is much more facile than the other, if the percentage yield for the slower reaction can be determined. This situation arises in the case of chemiluminescent (CL) reactions possessing low quantum yields (eq 1). The yield of photons and the determination of the rate constant for disappearance of A and/or appearance of B provide sufficient information to allow the determination of the rate law for the formation of $C^{\ddagger}$. This approach has been employed in the previous (see Introduction of ref 1) and present study.

## Experimental Section

**Materials.** ***N,N'*-Dimethyl-9,9'-biacridinium nitrate (1)** (Aldrich Chemical Co.) was repeatedly recrystallized from ethanol-water (5/95 v/v) to give orange crystals that were dried at 100 °C (0.1 mmHg) for 24 h: mp 250 °C dec; UV-vis (water, pH 3.72) 453 nm (log $\epsilon$ 3.93), 430 (4.03), 420 (3.95), 369 (4.55), 354 (4.24), 260 (5.22). ***N*-Methylacridone (2)** (Aldrich Chemical Co.) was recrystallized (three times) from absolute ethanol to give yellow crystals (needles) that melted at 210–211 °C (lit.[7] 209–210 °C). ***N,N'*-Dimethyl-9,9'-biacridylidene (3)** was obtained by reduction of **2** with zinc dust in alcoholic HCl.[8] Recrystallization from pyridine gave yellow crystals that melted above 360 °C, *m/e* ($M^+$) 386. ***N,N'*-Dimethyl-9,9'-biacridylidene 9,9-oxide (4)** was obtained by treatment of **1** with 40% sodium hydroxide in methanol, followed by successive washing of the resulting precipitate with methanol, water, and methanol.[9] Recrystallization from pyridine gave yellow crystals that melted at 259–261 °C (lit.[9] 260–262 °C). ***N,N'*-Dimethyl-9,9'-dihydroxybiacridan (5)** was obtained by the method of Lehmstedt and Hundertmark,[10] mp 285–290 °C (lit.[10] 300 °C). ***N*-Methylacridanol (6)** was obtained by the method of Krohnke and Honig,[7] mp 160–163 °C (lit.[7] 163–164 °C). ***N*-Methylacridan** (7) was obtained by the method of Pictet and Patry,[11] mp 99 °C (lit.[11] 96 °C). **Superoxide dismutase** (bovine) and **bovine serum albumin** were purchased from Sigma Chemical Co.

**Reagents and solvents** were all analytical or spectroscopic grade and used as obtained. Trifluoroethanol was distilled prior to use. Deionized and doubly distilled water was employed for the preparation of all kinetic solutions. Trace metals were removed from selected solutions with Chelex-100 cation exchange resin.

**Apparatus.** Ultraviolet and visible spectra and absorbance measurements were recorded on Cary 15, 116, or 118 spectrophotometers. Measurements of pH were performed with a Radiometer Model 26 pH meter equipped with Model EA-125 (Metrohm) or GK-2302C

0002-7863/79/1501-5355$01.00/0 

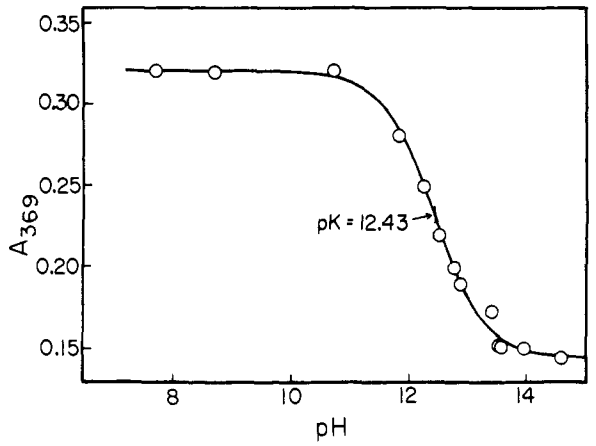


**Figure 1.** Spectrophotometric titration curve for pseudobase formation from **1**.

(Radiometer) electrodes. High-pressure liquid chromatographic analyses were carried out on a Lichrosorb reverse phase (10 × 250 nm, 10-$\mu$ particles) column using a Schoeffel Instrument SF 770 spectroflow monitor equipped with an Altex solvent metering system Model 100 and a Varian Associates CDC 101 integrator. Photon counting was carried out with Model 1140A Princeton Applied Research quantum photometers equipped with 1P28A photomultiplier tubes (30 °C). Analyses of all data were performed with the aid of either an iterative reaction kinetics simulator PDP 11/03 (Tektronix) or a Hewlett-Packard calculator Model 9825 equipped with Model 9862A plotter. Melting points were taken with a Thomas-Hoover capillary melting point apparatus and are uncorrected. Polarographic studies were carried out on a modified Princeton Applied Research Model 172 polarographic analyzer. Solutions were deoxygenated by passing a stream of $N_2$ through them for 0.5 h. Half-wave potentials were measured in aqueous solutions relative to a saturated calomel electrode at 25 °C with a dropping mercury electrode.

**Methods.** Spectrophotometric runs were performed on 3.10 mL of reaction mixture (containing $Na_2EDTA$, $10^{-4}$ M, $\mu$ = 1.0, 30.0 °C and $1.75 \times 10^{-5}$ M lucigenin) using a Gilford spectrophotometer at 369 nm. Phosphate (pH 11.3–13.3), trifluoroethanol (pH 11.3–13.3), and KOH (pH >13.3) were used as buffers. Measurements of CL emission were performed on 5.1 mL of the reaction solutions prepared in the same manner as the spectrophotometric runs. All reactions were studied in water at 30 °C and $\mu$ was maintained at 1.0 in all reactions excepting those carried out with $[HO^-] > 1.0$. All experimental points and table listings are the average of at least three individual measurements.

**Time Course for the Formation of Radical in the Reaction of Hydroxide Ion and Trifluoroethanol with 1.** After the mixing of buffer solution and **1** an aliquot of the reaction solution was immediately transferred into an ESR tube (the process required ~60 s) and the formation of radical followed by repetitive scanning the EPR spectrum and by following the appearance and disappearance of radical at a fixed field strength (3240 G for $HO^-$ reactions). For measurements under anaerobic conditions the solutions were deoxygenated by freeze–pump–thaw cycles under nitrogen. The solutions were then transferred into a drybox maintained under a nitrogen atmosphere where the reaction solutions were prepared and transferred to ESR tubes.

**Analysis for Products Obtained on Reaction of 1 with $HO^-$.** Lucigenin (**1**, 650 mg) was dissolved in 150 mL of phosphate buffer at pH 13.0 ($Na_2EDTA$, $10^{-4}$ M). The solution was then allowed to stand overnight in the dark. The reddish-brown precipitate was extracted into 50 mL of dichloromethane and the aqueous layer was further washed (2 × 50 mL) with dichloromethane. The washings were combined, dried ($MgSO_4$), and evaporated to dryness to leave a reddish-brown precipitate. An electron resonance spectrum of a solution of the precipitate ($CHCl_3$ solvent) gave a one-line signal that could not be resolved. The line width measured from maximum to minimum was 20 G. When 10 mg of the product mixture was dissolved in 3 mL of chloroform and then injected into the Lichrosorb reverse phase column (10 × 250 mm) followed by elution with chloroform (3 mL/min), the following compounds were isolated: *N,N'*-dimethyl-9,9'-dihydroxybiacridan (**5**), *N,N'*-dimethyl-9,9'-biacridylidene oxide (**4**), *N,N'*-dimethyl-9,9'-biacrylidene (**3**), *N*-methylacridone (**2**), *N*-methylacridanol (**6**), and *N*-methylacridan (**7**). The identities of the componerts in the various fractions were established by comparison of their UV and IR spectra and their retention times with those of authentic samples synthesized by independent means. Compounds **2**, **3**, **4**, **5**, **6**, and **7** were found to have retention times of 11.5, 9.0, 7.4, 6.8, 16.3, and 19.5 min, respectively, identical with the first six fractions obtained by LC. The yields of the various compounds were determined from the relative peaks areas.

**Table I.** Dependence of Half-Wave Potentials (vs. SCE) for Lucigenin Reduction upon pH (Initial Concentration of Lucigenin $1.72 \times 10^{-4}$ M; Electrolyte 0.10 M KCl; $T$ = 22 °C)

| pH | $E_{1/2}(1)$ | $E_{1/2}(2)$ | $E_{1/2}$(sh) |
|---|---|---|---|
| 0.70 | −0.22 | −0.37 | |
| 0.90 | −0.22 | −0.37 | |
| 1.50 | −0.21 | −0.38 | |
| 1.80 | −0.21 | −0.37 | |
| 1.96 | −0.22 | −0.38 | |
| 2.15 | −0.22 | −0.38 | |
| 6.37 | −0.21 | −0.38 | |
| 7.10 | −0.21 | −0.38 | |
| 8.90 | −0.21 | −0.37 | |
| 10.80 | −0.21 | −0.37 | |
| 12.95 | −0.20 | −0.36 | |
| 12.95[a] | −0.20 | −0.37 | −0.26 |
| 13.25 | −0.19 | −0.37 | −0.28 |
| 13.70 | | | −0.28 |

[a] Potential taken 10 min after pH was adjusted to 12.95.

## Results

Despite the implication of the involvement of pseudobase species of **1** in its CL reactions[3a] there have been no reported attempts to determine the values of $K_{a1}$ and $K_{a1}$ of eq 2.

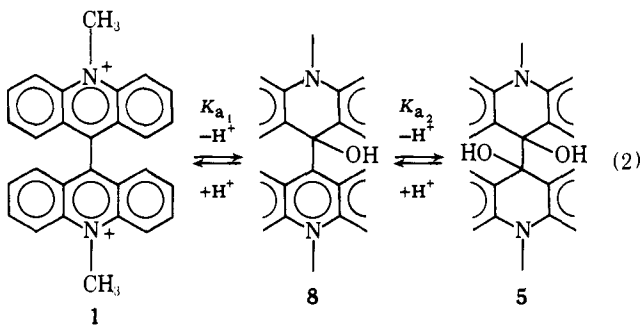


(2)

Spectrophotometric titrations of aqueous solutions of **1** were carried out at 368 nm. Between pH 3 and 11 there was noted to be no discernible change in $A_{368}$. Above ~pH 11 ($[\mathbf{1}] = 1 \times 10^{-6}$ to $9.76 \times 10^{-6}$ M) an increase in $A_{368}$ could be recorded and a plot of $A_{368}$ vs. pH was found to fit the theoretical curve for a single proton ionization (Figure 1) associated with a $pK_a$ of 12.43. With time the absorbances of alkaline solutions of **1** decrease. This decrease in absorbance becomes particularly marked above pH 13. Since the change in $A_{368}$ on titration from neutrality to pH 13 amounts to an absolute absorbance change of only 0.1 absorbance unit (10%), the decrease in absorbance with time above pH 13 prevents titration to higher pH values. Titration between pH 7 and 13 is reversible but above pH 13 reacidification does not completely regenerate the spectrum of **1**. These titrimetric results suggest that the $pK_{a1}$ of eq 2 equals 12.43 and that as $pK_{a2}$ is approached a partially irreversible reaction occurs.

**Dependence of the half-wave potentials for reduction of 1 on pH** was determined in buffered aqueous solutions (Table I). Between pH 0.70 and 10.80 the two half-wave potentials for reduction of **1** are readily discernible and independent of pH. Also, independent of the pH, in this range, is the concentration of **1** as determined from the differential pulse polarographic

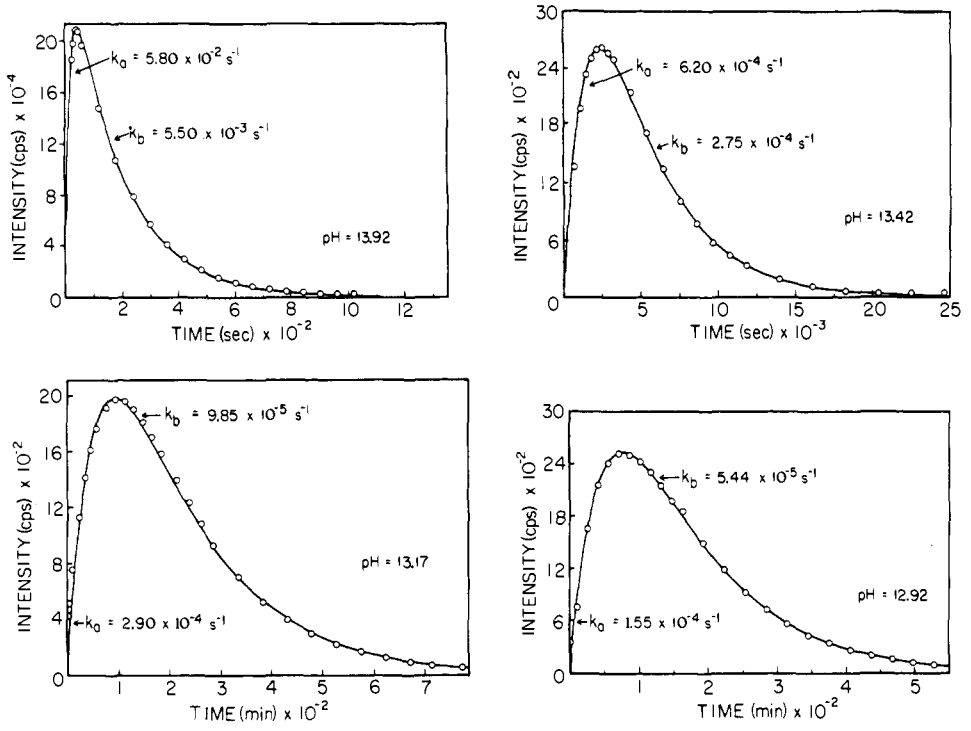


**Figure 2.** Computer fits of the consecutive first-order rate equation to the buildup and decay of photon emission.

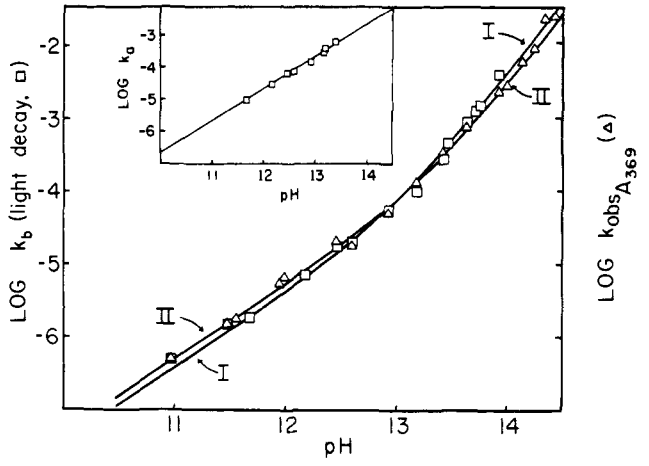


**Figure 3.** pH-log (rate) profiles for reaction with hydroxide (aerobic) from spectrometric rates ($k_{obsd}(A_{369})$, Δ, curve II) and rates of decay of light ($k_b$, □, curve I). Inset: pH-log $k_a$ profile for increase in CL intensity.

heights for $E_{1/2}(1)$ and $E_{1/2}(2)$. This suggests that the dication of **1** remains stable in aqueous solution up to at least pH 10.80. Hence, the spectrophotometrically determined p$K$ can only be p$K_{a1}$ of eq 2.

After 1 h at pH 12.95 the $E_{1/2}(2)$ peak completely disappeared with the appearance of a new peak (shoulder at −0.26 V). Further increase in pH to 13.70 resulted in complete disappearance of all pulsed polarographic peaks between 0 and −0.75 V. This result suggests the disappearance of **1** and **8** at high pH, confirming the spectroscopic observations made during the titration of **1**.

**The kinetics of light emission** were routinely studied with the initial concentration of **1** at $1.74 \times 10^{-5}$ M and $O_2$ at ca. $1.5 \times 10^{-4}$ M. At all hydroxide ion concentrations employed (pH 11 to 4 M) the photons emitted per second (cps) increased to a maximum value and then decreased. Below pH 11 the light emission was too weak to be accurately recorded by our instruments. Both the increase and decrease in cps were found to be exponential. The apparent consecutive first-order reactions for buildup of light intensity ($k_a$) and decay of light intensity ($k_b$) (Figure 2) can result from the system shown in eq 3, where $k_a = k_x + k_{-x}$ and $k_y > k_b < k_{-x}$. A plot of log $k_a$

$$\mathbf{1} \underset{k_{-x}}{\overset{k_x}{\rightleftharpoons}} \mathrm{A} \xrightarrow{k_y} \mathrm{C} + h\nu \qquad \mathrm{A} \xrightarrow{k_b} \mathrm{B} \tag{3}$$

vs. pH is shown in the inset to Figure 3, and the plot of $k_b$ vs. pH is shown as curve I of Figure 3. The line through the experimental points of the inset to Figure 3 was generated using eq 4. The constants employed to fit the experimental data are $k_1 = 5.0 \times 10^{-3}$ M$^{-1}$ s$^{-1}$ and $K_w = 13.78$. The line through the points of Figure 3 curve I was generated using eq 5, where $k_1 = 2.6 \times 10^{-4}$ M$^{-1}$ s$^{-1}$ and $k_2 = 1.8 \times 10^{-3}$ M$^{-2}$ s$^{-1}$.

$$k_a = k_1\left(\frac{K_w}{a_H}\right) = k_1[\mathrm{HO}^-] \tag{4}$$

$$k_b = k_1\left(\frac{K_w}{a_H}\right) + k_2\left(\frac{K_w}{a_H}\right)^2 = k_1[\mathrm{HO}^-] + k_2[\mathrm{HO}^-]^2 \tag{5}$$

**The rates of disappearance of 1** from solution were followed by repetitive spectral scanning between 300 and 500 nm at any constant pH (Figure 4). Sharp isosbestic points occurred at 347, 358, 364, 382, 394, and 480 nm. A plot of $A_{326}$ vs. time could be accurately fit by the equations for consecutive first-order reactions:

$$\mathrm{A} \xrightarrow{k_a'} \mathrm{B} \xrightarrow{k_b'} \mathrm{C} \tag{6}$$

In 1.0 M KOH, for example, $k_a'$ and $k_b'$ were determined to be $2.07 \times 10^{-4}$ and $2.23 \times 10^{-5}$ s$^{-1}$. At lower concentrations of hydroxide (pH 10-13.5) $A_{326}$ increased with time and then became almost constant for an extended period of time. The eventual decrease in $A_{326}$ was found to parallel the disappearance of a radical signal. The increase in $A_{326}$ with time provided the same first-order rate constants as obtained by employing $A_{369}$. The reaction when monitored at 369 nm was found to follow first-order kinetics for 4 half-lives between pH 10.50 and 13.80 and ca. 2.5 half-lives from 1.0 to 4.0 M KOH.

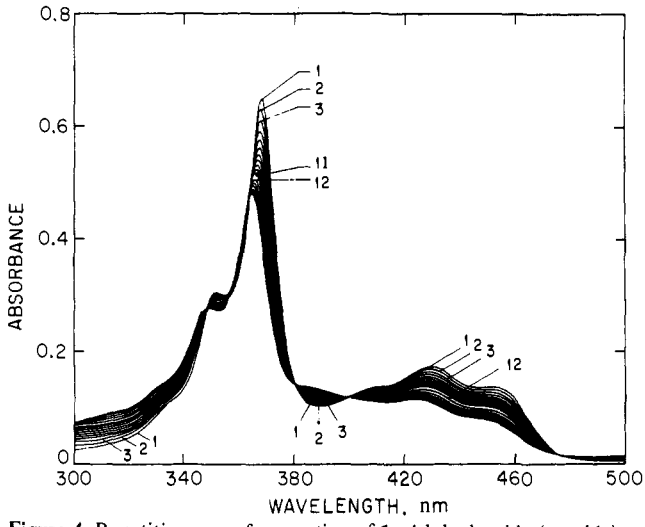


**Figure 4.** Repetitive scans for reaction of **1** with hydroxide (aerobic) at pH 13.64. Time interval between scans 1 and 2 is 157 s, and 500 s for all other scans. Lucigenin concentration, $1.75 \times 10^{-5}$ M.

**Table II.** Comparison of Rate Constants (eq 5) for Exponential Decay of Light Emission and Disappearance of **1**

| | $k_1$, $M^{-1} s^{-1}$ | $k_2$, $M^{-2} s^{-1}$ |
|---|---|---|
| *hν* decay | $2.6 \times 10^{-4}$ | $1.8 \times 10^{-3}$ |
| disappearance of **1** | $3.4 \times 10^{-4}$ | $1.2 \times 10^{-3}$ |

Figure 3 (curve II) is a plot of the logarithm of the pseudo-first-order rate constant for disappearance of **1** ($k_{obsd}$) as determined at 369 nm vs. pH. The line which fits the experimental points has been generated from eq 5. Thus, the same rate equation pertains to the disappearance of **1** and to the exponential decay of light emission (i.e., **1** → B of eq 3 with associated constant $k_b$). In fact the rate constants $k_1$ and $k_2$ of eq 5 are found to be very similar for disappearance of **1** and exponential decay of light production (Table II). This finding suggests that the rate-determining step(s) for both processes are the same, i.e., that the major non-CL path controls the kinetics (see Introduction).

The chemiluminescence spectra of the reaction of **1** with hydroxide in the presence of $O_2$ and at various concentrations of **1** are shown in Figure 5. A decrease in the concentration of **1** resulted in a shift of the CL spectrum toward shorter wavelengths. This is consistent with modification of CL emission from excited *N*-methylacridone (**2**) due to absorption by **1**, as seen in the reaction of **1** with hydrogen peroxide.[1]

**The dependence of the chemiluminescent quantum yield on pH** is provided in Figure 6. The quantum yields ($\Phi_{CL}$) of Figure 6 were determined by integration of the area under the plots of cps vs. time. Comparison of Figures 3 and 6 establishes that the quantum yield exhibits a zero-order dependence upon [$HO^-$] whereas reaction of **1** and exponential decay of light exhibit a first- and second-order dependence upon [$HO^-$] (eq 5). These results suggest that, though the major reaction(s) of **1** (which are non-light-producing) control the rates of disappearance of **1** (and formation of the excited species), the minor and therefore non-rate-determining CL processes are of the same order in [$HO^-$] as are the major reactions. The rates of the major reaction paths and the CL reaction differ, however, in their dependence upon [**1**]. Thus, the quantum yield was found to be dependent upon the initial concentration of lucigenin. Figure 7 shows that there is an approximate first-order dependence of $\Phi_{CL}$ upon [**1**] between pH 11.5 and 4 M $HO^-$. This result establishes that two molecules of **1** are required for the formation of each photon in the CL reaction.

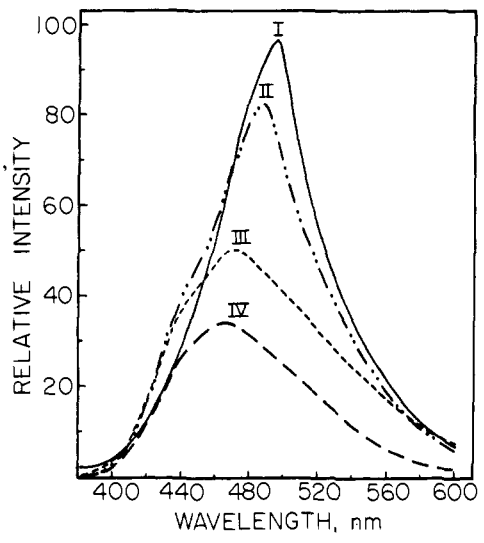


**Figure 5.** Chemiluminescence spectra of reaction with hydroxide (aerobic) in 1.0 M KOH at lucigenin concentrations of $1.57 \times 10^{-4}$ (curve I), $5.95 \times 10^{-5}$ (curve II), $2.30 \times 10^{-5}$ (curve III), and $1.06 \times 10^{-5}$ M (curve IV).

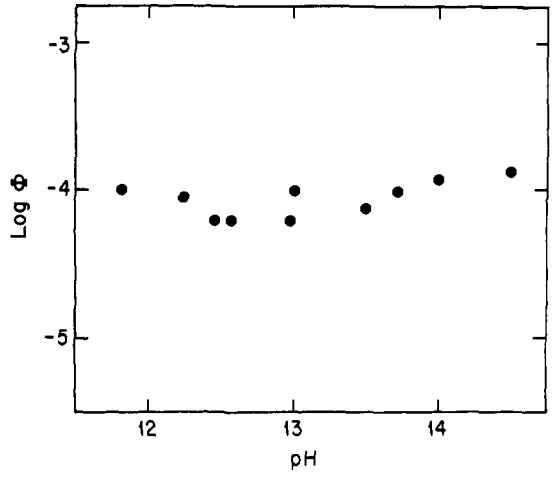


**Figure 6.** Logarithm of quantum yield vs. pH for the reaction of hydroxide ion with **1** ($1.75 \times 10^{-5}$ M).

**Radical formation in the reaction of lucigenin with hydroxide ion** was followed by ESR spectroscopy. A single-line ESR spectrum of 14.5 ± 1.5 G peak-to-peak width and 2.011 *g* value was observed at 298 K when [**1**] = $1.45 \times 10^{-4}$ to $1.75 \times 10^{-5}$ M and at pH values between 12.50 and 14. Attempts at separating the radical(s) from other reaction products either by fractional crystallization or high-pressure liquid chromatography resulted in loss of the ESR signal. Figure 8 depicts the spectrum obtained at pH 13.55 at 298 K under anaerobic conditions. When extracted from the reaction mixture with $CHCl_3$ the radical(s) was found to be stable (in the solid state) for 3 months without any sign of decomposition. In solution, however (acetonitrile, dioxane, and tetrahydrofuran), the radical was not as stable. For example, in acetonitrile solution the ESR signal intensity decreased by 70% in 24 h.

The time course of radical generation and disappearance was followed (298 K) at either a constant field strength of 3240 G (position of one of the peaks in the ESR spectrum) and a microwave frequency of 9.16 GHz or by repetitive scanning of the radical spectrum over a range of 100 G. Curve I of Figure 9 and the inset represent the change in ESR signal vs. time determined at pH 13.5 with an initial [**1**] = $6.59 \times 10^{-5}$ M. At higher [**1**] ($5 \times 10^{-4}$ M) deposition of a brown precip-

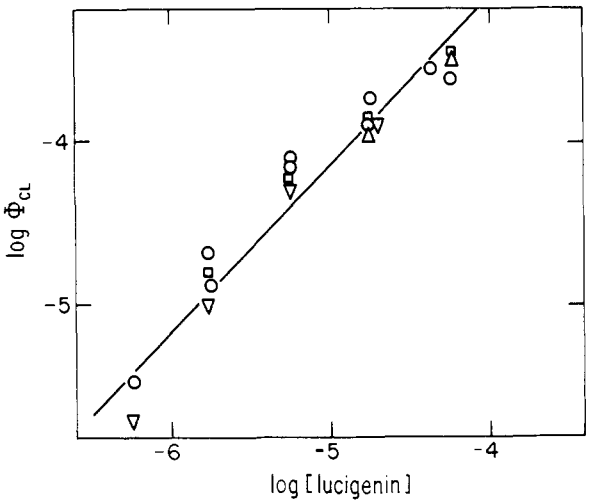


**Figure 7.** Logarithm of quantum yield vs. log [**1**] for the reaction of **1** with hydroxide ion at pHs 11.8 (△), 13 (□), and 14 (○), and at 5 M KOH (▽).

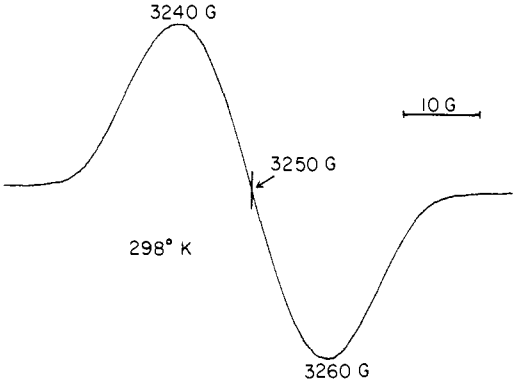


**Figure 8.** ESR spectrum for the radical(s) from the reaction of lucigenin with hydroxide at pH 13 under anaerobic conditions.

itate occurred. Examination of Figure 9 reveals that the appearance of the ESR signal exhibits a small lag period of about 10 min followed by a first-order increase to a maximum intensity. The intensity then remained constant for ca. 3–4 h before slowly decaying to zero (see inset). Figure 9 also allows comparison of the time course of the CL reaction (integrated intensity vs. time, curve II), the disappearance of **1** observed spectrophotometrically (absorbance vs. time, curve III), with the time course of the radical formation (curve I). Curves I and II may be seen to resemble each other very closely. That is, the radical accumulates during the CL reaction. The lag phase in the appearance of both radical and light emission and the increase in radical concentration until light emission processes are complete suggest that the radical is an intermediate which could be formed along the CL reaction pathway.

When radical concentration reached a steady-state concentration (constant ESR signal) the addition of a drop of concentrated hydrochloric acid led to a complete disappearance of the ESR signal. Rebasification regenerated the same ESR spectrum. Oxygen (i.e., air) apparently has no influence on either the formation or the stability of the radical(s), at least not over a 30-min period (relative to the radicals observed under anaerobic conditions). Addition of a drop of 30% hydrogen peroxide results, however, in the immediate disappearance of the ESR signal.

**The isolatable end products from the reaction of lucigenin with hydroxide ion** under both aerobic and anaerobic conditions are *N*-methylacridone (**2**), *N,N'*-dimethyl-9,9'-biacrylidene (**3**), *N,N'*-dimethylacrylidene oxide (**4**), *N,N'*-dimethyl-

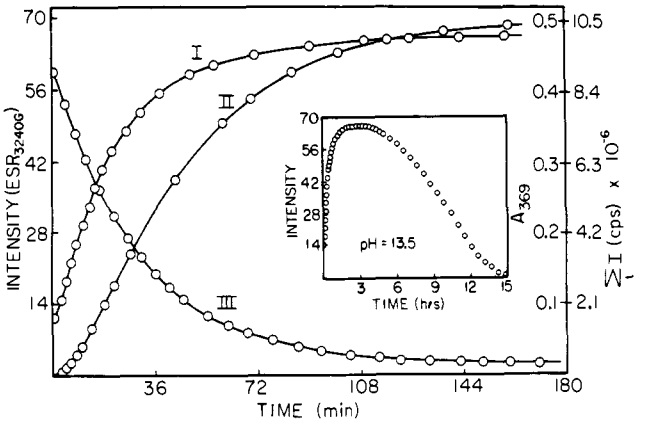


**Figure 9.** Plots of intensity of ESR signal vs. time (curve I), relative integrated light intensity vs. time (curve II), and absorbance (369 nm) vs. time (curve III) for reaction of lucigenin with hydroxide (aerobic) at pH 13.5. Inset: complete time course for the formation and decomposition of the radical ESR signal at pH 13.5.

**Table III.** Relative Yields of the Products of the Reaction of Lucigenin with Hydroxide Ion (pH 13, $H_2O$ Solvent, 30 °C, Aerobic)

| compd | % yield | method |
|---|---|---|
| **2** | 25 | *a, b* |
| **3** | 10 | *a, b* |
| **4** | *15* | *a, b* |
| **5** | 25 | *a* |
| **6** | 5 | *b* |
| **7** | 5 | *b* |

[a] Analysis by LC (see Experimental Section). [b] By isolation using column chromatography on silica gel.

9,9'-dihydroxybiacridan (**5**), *N*-methylacridanol (**6**), and *N*-methylacridan (**7**). The products were identified (see Ex-

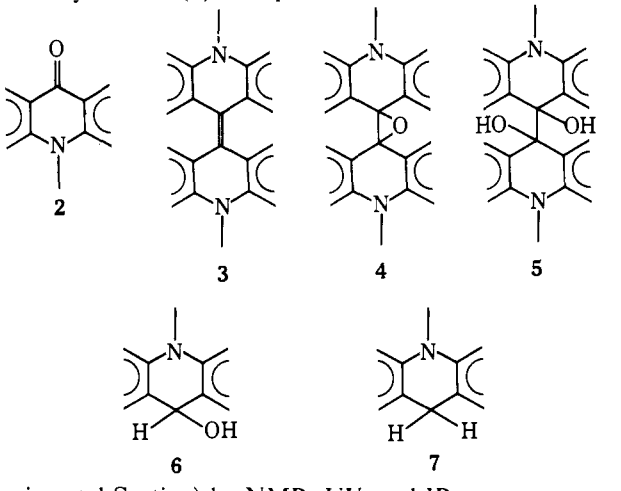


perimental Section) by NMR, UV, and IR spectroscopy as well as by chromatography. The percentage yields of each product (pH 13) based on the initial concentration of **1** are provided in Table III. The yields provided in Table III may not truly represent the composition of the kinetic reactions at completion since some of the products are quite labile. Products such as **4** and **5** may be reconverted to **1** on acidification. From Table III the summed percent yield of **4** and **5** amounts maximally to 40%. It has been noted by previous investigators[12] that not all of **1** is consumed during the CL reaction. What actually occurs is that **1** is converted, in part, to labile compounds, such as **4** and **5**, which are easily reconverted to **1**. Concentrations of these "storage forms" of **1** may be conveniently determined by use of the CL reaction of

Table IV. Chemiluminescent Intensities Resulting from Various Combinations of **1**, **3**, **4**, and $O_2$

| soln composition[a] | init intensity[b] |
|---|---|
| **1** + $O_2$ | $<1 \times 10^5$ |
| **3** + $O_2$ | $<1 \times 10^5$ |
| **4** + $O_2$ | $<1 \times 10^5$ |
| **1** + **3** | $5.3 \times 10^6$ |
| **1** + **4** | $5.1 \times 10^6$ |
| **1** + **3** + $O_2$ | $8.8 \times 10^9$ |
| **1** + **4** + $O_2$ | $1.1 \times 10^{10}$ |

[a] [**1**] = $5 \times 10^{-4}$ M, [**3**] = $1 \times 10^{-5}$ M, [**4**] = $1 \times 10^{-5}$ M, all in MeOH. [b] Photons per second. All reactions had half-lives ranging from $5 \times 10^4$ to $8 \times 10^4$ s.

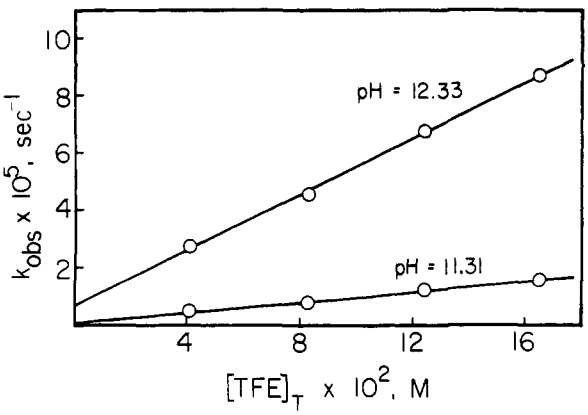


Figure 10. Plot of pseudo-first-order rate constants for CL decay vs. total concentration of trifluoroethanol at pH 11.31 and 12.33 with $1.75 \times 10^{-5}$ M lucigenin.

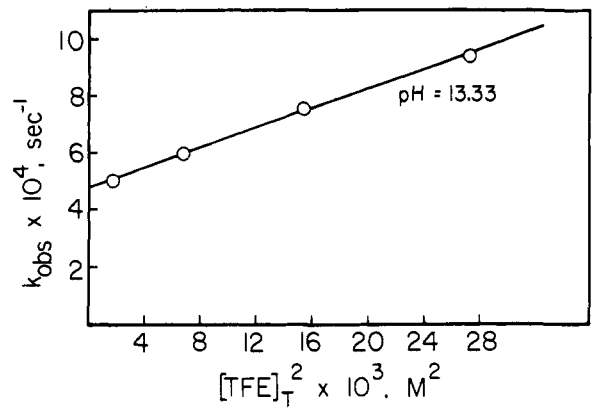


Figure 11. Plot of pseudo-first-order rate constants for CL decay vs. square of total TFE concentration at pH 13.33 with $1.75 \times 10^{-5}$ M lucigenin.

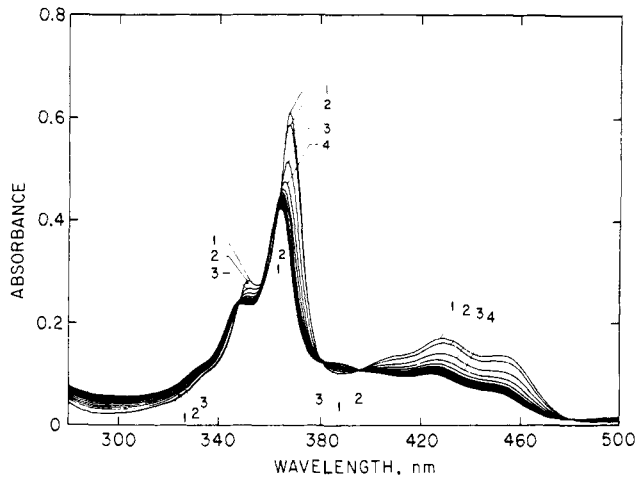


Figure 12. Repetitive scans for reaction of lucigenin with TFE at pH 12.33. [TFE] = 0.165 M; [lucigenin] = $1.75 \times 10^{-5}$ M. Time interval between any two consecutive scans is 20 min.

**1** with hydrogen peroxide.[1] The addition of basic hydrogen peroxide to an acidified (pH 3-5) spent reaction of **1** in aqueous solution produces an intense CL. This CL reaction may be employed to assess the percent yield of products reconvertible to **1** by comparing the $\Phi$ for the peroxide assay to the quantum-yield values obtained when employing standard solutions of **1** as the CL agent. The results of these experiments showed that approximately 50% of **1** is regenerated upon acidification of the spent solutions for reactions carried out at pH 13.

**The role of comproportionations between 1 and various reduced forms of 1** such as **3** or **4** in the CL reaction was examined by reacting solutions of **1**, **3**, and **4** in MeOH. Table IV shows that, while upon addition of $O_2$ to separate solutions of **1**, **3**, and **4** little chemiluminescence was observed, the addition of $O_2$ to solutions of **1** + **3** or **1** + **4** resulted in intense chemiluminescence and $\Phi_{CL}$ exceeding those observed on reaction of **1** with $HO^-$ in the presence of $O_2$. The CL pathway therefore requires (1) both **1** and molecules which can transfer $1e^-$ to **1** and (2) molecular $O_2$.

**Reaction of 2,2,2-Trifluoroethoxide with 1.** If the addition of $HO^-$ to **1** is an important feature of the CL reaction then the addition of alkoxide ions to **1** should also result in CL unless dissociation of the hydroxyl group(s) proton(s) of the adduct is required. Trifluoroethanol (TFE) was chosen for mechanistic studies because of its relatively low $pK_a$ (12.45)[13] in aqueous solution.

The reaction of **1** with TFE in basic solutions (pH 10.40, 11.31, 12.33, and 13.33) leads to an intense CL. In the presence of TFE an initial buildup in light emission is followed by an exponential decay similar to that seen for the reaction of **1** with $HO^-$. The pseudo-first-order rate constants obtained from the exponential decrease in the intensity of light emission are a linear function of $[TFE]^1$ at pH 10.40, 11.31, and 12.33 (Figure 10) but exhibit a dependence upon $[TFE]^2$ at pH 13.33 (Figure 11). Repetitive scans of the reaction exhibited isosbestic points (348, 356, 363, 380, 397, 480 nm) which are at positions almost the same as those obtained in the reaction of hydroxide ion with **1**. A typical repetitive scan is shown in Figure 12. The close resemblance between Figures 4 and 12 suggests formation of structurally similar intermediates in the two reactions. In addition the major fluorescent product formed during the course of both reactions is **2**.

The rate of disappearance of **1**, observed at 368 nm at pH 11.31, 12.33, and 13.33, followed first-order kinetics for at least 3.5 half-lives. The dependence of the pseudo-first-order rate constants upon [TFE] was the same as that obtained from the CL reaction, that is, first order in [TFE] at pH 11.31 and 12.33 and second order at pH 13.33.

**The dependence of quantum yields upon pH and [TFE]** was found to be quite different than in the case of the reaction of **1** with $HO^-$. Thus, the quantum yields decrease with increasing pH in experiments employing initial [**1**] = $6.5 \times 10^{-6}$ M and with [TFE] varying from $4.09 \times 10^{-2}$ to 0.25 M. The determined values of $\Phi_{CL}$ are tabulated in Table V. At pH 13.33 the values are the same with and without TFE. The values of $\Phi_{CL}$ at pH 13.33 are very close to those seen in the absence of TFE. Examination of the data of Table V reveals that $\Phi_{CL}$ is virtually independent of [TFE] at any constant pH.

**The reaction of lucigenin with TFE also produced radical(s)** at concentrations easily detectable by ESR. At pH 13.33, lucigenin concentration of $1.75 \times 10^{-5}$ M, and TFE concen-

**Table V.** Dependence of Quantum Yields upon Concentration of TFE at Various pHs

| $[TFE]_T \times 10^2$, M | quantum yield $\Phi_{CL} \times 10^5$ | | |
|---|---|---|---|
| | pH 10.40 | pH 12.33 | pH 13.33 |
| 4.09 | 34 | 16 | 2.4 |
| 8.17 | 41 | 33 | 3.6 |
| 12.28 | 57 | 33 | 4.3 |
| 16.34 | | 34 | 5.1 |
| 24.55 | 40 | | |

**Table VI.** Effect of Various Nucleophiles at Constant pH upon Chemiluminescent Reaction Rates and Quantum Yields

| | [nucleophile] | $k_b$, $s^{-1}$ | $\Sigma I$, cps |
|---|---|---|---|
| pH 11.50 | $3.2 \times 10^{-3}$ M KOH | $3.4 \times 10^{-6}$ | $2.0 \times 10^{18}$ |
| | $1 \times 10^{-2}$ M $EtNH_2$ | $1.65 \times 10^{-5}$ | $2.2 \times 10^{18}$ |
| pH 12.50 | $3.2 \times 10^{-2}$ M KOH | $2.48 \times 10^{-5}$ | $2.9 \times 10^{18}$ |
| | $3.2 \times 10^{-2}$ M $EtNH_2$ | $3.16 \times 10^{-5}$ | $2.1 \times 10^{18}$ |
| | $3.2 \times 10^{-2}$ M KCN | $1.28 \times 10^{-4}$ | $9.0 \times 10^{18}$ |

tration of $4.09 \times 10^{-2}$ M, the spectrum consisted of a single line with peak-to-peak width of 1.6 G and $g$ value of 2.012. The signal, except for the narrower width, was the same as that for the radical from the hydroxide reaction. The same spectrum was obtained at pH 12.33. Lowering of temperature to 203 K resulted in lower intensity but the same width.

The following *similarities and differences* have been found *for the reactions of trifluoroethoxide and hydroxide:* (1) the repetitive scans in the UV and visible wavelengths are almost identical; (2) below pH 13 the rate of disappearance of **1** is first order with respect to each nucleophile and above pH 13 it becomes second order; (3) the quantum yields are higher at low pH in TFE solutions but at high pH the quantum yields fall to the value seen in the absence of TFE; (4) the quantum yields are independent of the nucleophile concentration at a given pH; (5) the rates of disappearance of **1** are greater in the presence of TFE at any constant pH; (6) radicals with similar EPR signals are produced with and without TFE.

**Nucleophiles other than hydroxide and trifluoroethoxide** were found to react with **1** (Table VI). In the presence of ethylamine the initial intensity of light emission was greater than in its absence (lower pHs). However, the rate of exponential decay of light emission also increased so that $\Phi_{CL}$ was not substantially different than that obtained from hydroxide at the same pH. At higher pHs ethylamine affected neither the time course for light emission nor quantum yield. Comparison of cyanide rates and quantum yields relative to those for hydroxide shows that the former increases the rate of CL decay and intensity of maximum light emission leading to a small increase in quantum yield.

**The possible role of superoxide anion** on the course of the CL reaction was examined by addition of superoxide dismutase (SOD) to an aerobic solution of **1** in 1 M $CO_3^{2-}$ (pH 10.7), and by addition of potassium superoxide in THF to solutions of **1** (pH 13). The effect of SOD addition is shown in Table VII. In order to determine whether SOD decreases light due to removal of $O_2^{-}\cdot$ or whether the effect is due to binding of **1** to the enzyme, the effect of bovine serum albumin upon the CL reaction was also examined (Table VII). The effect of $KO_2$ addition is shown in Table VIII. Neither addition of SOD at pH 10.7 or $O_2^{-}\cdot$ at pH 13 affected the rate of CL decay.

**Table VII.** Effect of Superoxide Dismutase (SOD) and Bovine Serum Albumin (BSA) upon Maximum Light Intensity ($I_{max}$) in the Reaction of **1** with Hydroxide (1 M $CO_3^{2-}$, pH 10.7)

| [protein] | $I_{max}$, cps[a] |
|---|---|
| 0 | $12 \times 10^6$ |
| $5.7 \times 10^{-6}$ M SOD | $2.2 \times 10^6$ |
| $2.9 \times 10^{-5}$ M SOD | $4.5 \times 10^5$ |
| $1.5 \times 10^{-5}$ M BSA | $8.8 \times 10^5$ |

[a] Listed values are an average of three or four individual measurements.

**Table VIII.** Effect of Superoxide Anion ($O_2^{-}\cdot$) upon Maximum Light Intensity ($I_{max}$) in the Reaction of **1** with Hydroxide (pH 13)

| $[O_2^{-}\cdot]$ | $I_{max}$, cps[b] |
|---|---|
| 0[a] | $3.9 \times 10^9$ |
| $5.45 \times 10^{-7}$ M | $4.5 \times 10^9$ |
| $5.45 \times 10^{-5}$ M | $2.0 \times 10^9$ |

[a] Identical amounts of THF were present in all experimental runs (10% v/v). [b] Listed values are an average of three or four individual measurements.

## Discussion

It has been appreciated for some time that lucigenin (**1**) undergoes CL reactions with a number of chemical agents when in the presence of oxygen. For example, CL reactions have been reported to occur on reduction of **1** by alkaline fructose solutions,[2d] on reaction of **1** with xanthine–xanthine oxidase couple,[12] and upon the addition of various nucleophiles to **1**.[3a,4b] The chemiluminescent quantum yields ($\Phi_{CL}$) for these reactions are far below unity. For this reason any kinetic study which does not include a consideration of the dependence of $\Phi_{CL}$, as well as rate, upon variations in concentrations of reactants can only, at best, provide a description of the rate law for the non-CL reaction(s). This has not been appreciated in the study of CL reactions. Further, the kinetic investigations of the CL reactions of **1** have not resulted in the identification of the composition of critical transition states since the particular reactions chosen were often much more complicated than were necessary for CL. The roles of acid–base equilibria and hydroxide ion as a nucleophile were at times also ignored (no attention was paid to pH, etc.). In this study we have examined the kinetics and quantum yields of CL reactions resulting from the addition of nucleophiles to **1** under conditions which have minimized the number of unknown variables and allowed a systematic analysis of the results, i.e., at definite pHs, pseudo-first-order conditions, and employing the minimum number of reactant species required for chemiluminescence to occur.

Information concerning the mechanism of a CL reaction may be obtained by kinetic methods, even if the CL reaction is minor and in competition with major dark reactions, if rate constants for starting material conversion and light decay in the CL reaction are compared to quantum yields measured at the same reactant concentrations at which the rate constants were determined (see Introduction in preceding paper).

The pseudo-first-order rate constants for disappearance of **1** ($k_{obsd}$) and CL decay ($k_b$) show a first-order dependence upon $[HO^-]$ below pH 13 and a second-order dependence at pHs >13 (Figure 3). Since $\Phi_{CL}$ remains constant over the measured pH range (Figure 6), *both* the CL and non-CL reactions must be first order in hydroxide at pHs <13 and second order in $[HO^-]$ at higher pHs. (If only the CL reaction possessed a first-order dependence upon $[HO^-]$ (pH <13), $\Phi_{CL}$ would increase with increasing $[HO^-]$. If only the non-CL reaction possessed a first-order dependence upon $[HO^-]$, $\Phi_{CL}$ would decrease with increase in $[HO^-]$.) These data indicate that the CL and non-CL paths for conversion of **1** into products are kinetically identical in their dependence upon $[HO^-]$.

The rates of disappearance of **1** in the presence of ethylamine (pH 11.50) and cyanide (pH 12.50) are greater than in their absence at the given pH values. Also, the initial light intensities and rates of light decay are somewhat greater with these reagents. However, examination of Table VI shows that $\Phi_{CL}$ is not significantly affected by addition of these nucleophiles. Addition of trifluoroethanol increased both $\Phi_{CL}$ (comparison of Table V and Figure 6) and the rate of chemiluminescent decay (comparison of Figures 10, 11, and 3 at given pHs). At very high pHs (>13), however, both $k_b$ and $\Phi_{CL}$ measured in the absence and presence of TFE are very similar. The $pK_a$ of TFE is 12.43 and upon increase in pH the concentration of trifluoroethoxide will increase until its $pK_a$ is reached. Further increase in pH does not significantly increase [$TFE^-$] but does increase [$HO^-$]. Since the CL reaction is dependent upon [$HO^-$]$^2$ at high pH, chemiluminescence at pH >13 results from the hydroxide reaction. These facts suggest that the formation of adducts of **1** is of primary importance in the CL pathway while the nature of the nucleophile is of secondary import.

By comparison of the time courses for light emission and for disappearance of **1** it is possible to conclude that **1** must be converted to an intermediate which then undergoes a CL reaction. Thus, the decrease in [**1**] (368 nm) follows a simple first-order ($k_{obsd}$) rate law while the buildup of the intensity ($k_a$) and the decay of the intensity ($k_b$) of light emission follow consecutive first-order kinetics. The fact that the first-order rate constant for the buildup of light emission ($k_a$) is dependent upon [$HO^-$]$^{1.0}$ (inset to Figure 3) below pH 13 suggests that the addition of one $HO^-$ to **1** is required for CL. Since $\Phi_{CL}$ is independent of pH, both the CL reaction and non-CL reaction(s) must share this common step of $HO^-$ addition to **1**. The observation that $\Phi_L$ exhibits a first-order dependence upon **1** (Figure 7) establishes that the CL reaction is overall second order in **1** (if it were first order in **1**, $\Phi_{CL}$ would be independent of [**1**]). Two molecules of **1** or molecules derived from **1** are, therefore, required for the generation of each photon.

Chemiluminescence in the course of the reactions of **1** with bases under aerobic conditions may be due to radical reactions. Radicals have been detected during the course of CL reactions resulting from the addition of hydroxide[3a] and other bases[4b] to **1**. Radical formation in the course of addition of nucleophiles to acridinium salts appears to be a general phenomenon.[3b] In this study radical signals were observed upon addition of either $HO^-$ or trifluoroethanol (TFE) (at pH values approaching the latter's $pK_a$) to solutions of **1** under either aerobic or anaerobic conditions (Figure 8). The ESR spectra observed in this study differed from those detected by Janzen.[3a] This may be due to low solubility for the various radical species in pure water, with consequent complexing or aggregation of radicals, leading to loss of resolution and signal broadening.[14] Radical formation and CL may be related since both accumulation of quanta and radical intensity exhibit a lag phase, with subsequent identical rates of radical buildup and quanta accumulation (Figure 9).

The overall reaction of **1** with bases in the presence of $O_2$ provides a plethora of final products (Table III). These products all arise, however, through pathway(s) for which the critical transition state(s) contain one molecule of **1** plus one $HO^-$ ion at low pH and two $HO^-$ ions at high pH. The formation of the transition state for the rate-determining step of the CL reaction requires a minimum of two molecules of **1** and, as is the case of non-CL reactions, one $HO^-$ species at low pH and two $HO^-$ ions at high pH. Further, the excited product from the CL reaction is *N*-methylacridone (see Results).[1,2a] The simplest kinetically competent mechanisms for the CL reaction require, therefore, that the two transition states for the rate-determining steps of chemiluminescence be reached by the reaction, in some sequence, of 2 **1** + $HO^-$ and 2 **1** +

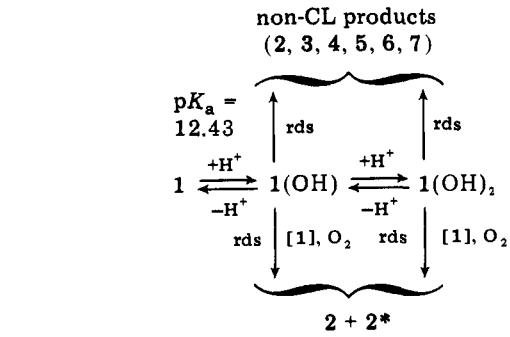


(7)

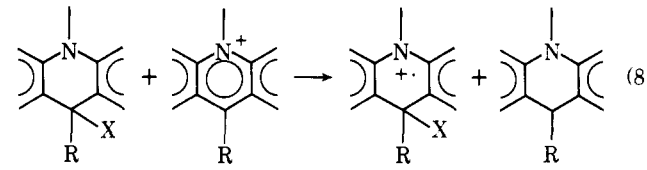

(8)

X = HO—, $CF_3CH_2O$—, $C_2H_5NH$—, H—

Scheme I

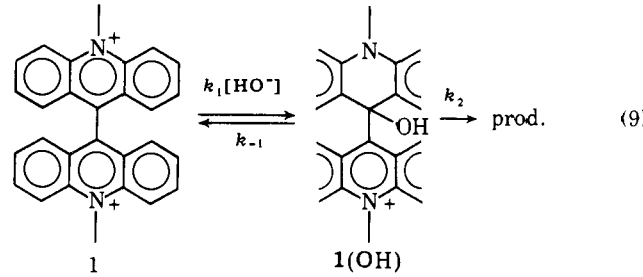


(9)

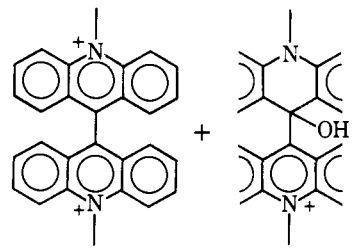

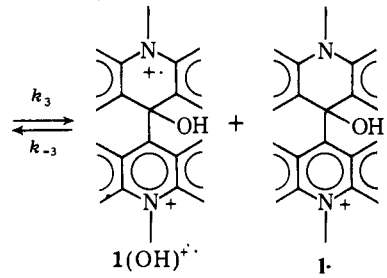


(10)

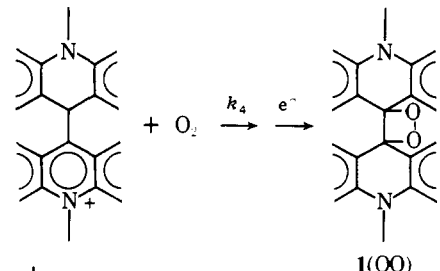


(11)

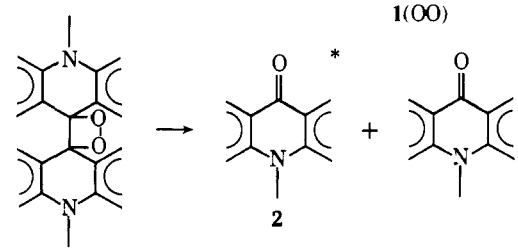


(12)

**Scheme II**

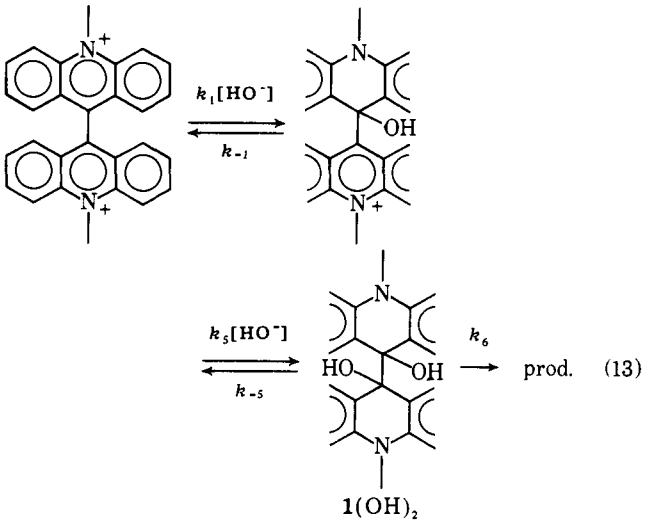


$$1\cdot + O_2 \xrightarrow{k_4} \xrightarrow{e^-} 1(OO) \longrightarrow 2 + 2^*$$

$2HO^-$, respectively, and that excited *N*-methylacridone is produced as the emitter. The formation of the critical transition states for the CL and non-CL reactions differs only in that the former reaction involves an additional molecule of **1** or species derived from **1**. It is reasonable that CL and non-CL reactions share, in part, a common pathway (eq 7).

The simplest of the kinetically acceptable mechanisms for chemiluminescence at low and high pH are provided in Schemes I and II respectively. The reaction sequences of Schemes I and II share in common the formation of pseudobases of **1** which, owing to their dihydroacridine structures, are capable of $1e^-$ transfer to **1**, providing radical species which then react with molecular oxygen to yield a dioxetane whose decomposition provides an excited state *N*-methylacridone (**2***). The comproportionation reactions proposed in Schemes I and II are quite reasonable since similar representative reactions such as those between **1** and **3** and between **1** and **4** under aerobic conditions produce an intense chemiluminescence (Table IV). Chemiluminescence obtained with other nucleophiles (i.e., $CN^-$, $CF_3CH_2O^-$, $C_2H_5NH_2$, etc.) would also involve $1e^-$ transfer from analogous nucleophilic adducts (which possess dihydroacridine structures, eq 8) to **1**. Chemiluminescence brought about by reduction of **1** by alkaline fructose could also involve $1e^-$ transfer from dihydroacridine intermediates (eq 8) to **1** again providing **1**·.[2d] Chemiluminescence may also result from comproportionations between various reaction products which could also provide the intermediate **1**· (Scheme III). Reactions in Scheme III such as eq 16 and 17 have been experimentally shown to produce chemiluminescence (Table IV).

**Scheme III**

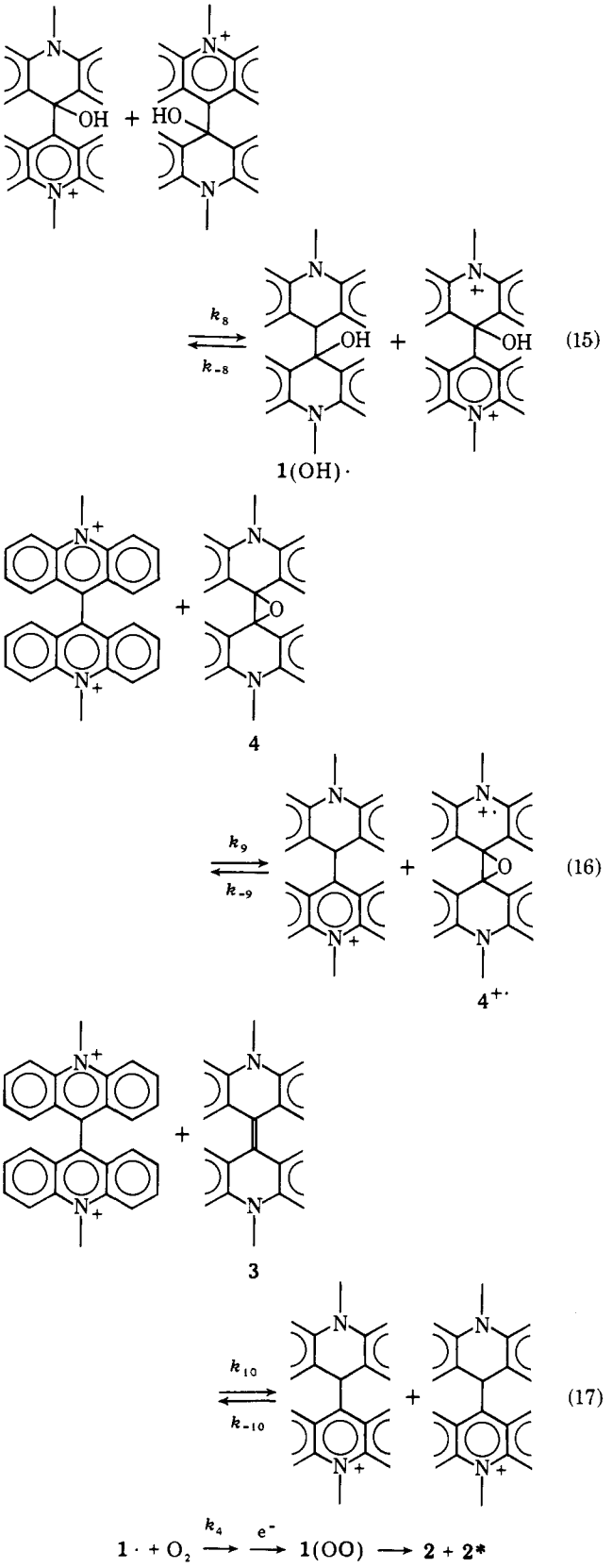


$$1\cdot + O_2 \xrightarrow{k_4} \xrightarrow{e^-} 1(OO) \longrightarrow 2 + 2^*$$

Assuming that $k_1, k_{-1}, k_5, k_{-5} > k_3, k_7, k_8, k_9, k_{10} > k_6 > k_2$ and that the other rate constants are fast, Schemes I–III

**Scheme IV**

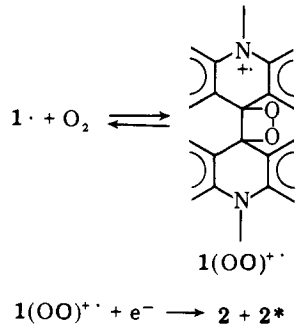


predict (1) a rate of disappearance of **1** which would possess a first-order dependence upon $[HO^-]$ at lower pHs and a dependence upon $[HO^-]^2$ at higher pHs; (2) identical rates for CL ($k_b$) and non-CL ($k_{obsd}$) reactions since the concentrations of CL pathway intermediates would be controlled by the concentrations of **1**, **1**(OH), and **1**$(OH)_2$; (3) both the CL reaction and buildup of radicals would be biphasic; (4) constant $\Phi_{CL}$ with increasing pH since both CL and non-CL paths involve one or two hydroxide additions; (5) a first-order increase in $\Phi_{CL}$ with increasing [**1**] since two molecules of **1** or its derivatives such as **1**(OH), **1**$(OH)_2$, **3**, or **4** are required in the comproportionation reactions (eq 10, 14–17); (6) radicals would be formed, some, such as **1**· and **1**(OH)· which have been previously detected and identified.[3a]

Legg and Hercules[5] have shown that the reaction of superoxide ($O_2^-$·) with **1** results in CL. A similar conclusion was reached by Fridovich[12] since CL had been observed upon the addition of **1** to a xanthine–xanthine oxidase system, which is known to produce $O_2^-$. We have found that addition of superoxide dismutase to a solution of **1** in aerobic 0.1 M carbonate (pH 10.7) decreased the amount of light produced (Table VII), but on the other hand so did the addition of bovine serum albumin. Superoxide could arise on reaction of molecular oxygen with the various radical species formed in the present system. Direct participation of $O_2^-$· in the CL reaction of this study could arise from the reactions

$$\mathbf{1}\cdot + O_2 \rightleftarrows \mathbf{1} + O_2^-\cdot \quad (18)$$

$$\mathbf{1}\cdot + O_2^-\cdot \rightarrow \mathbf{1}(OO) \rightarrow \mathbf{2} + \mathbf{2}^* \quad (19)$$

Addition of potassium superoxide to solutions of **1** at various pHs did not increase either maximum light intensity or quantum yield (Table VIII). A mechanism consistent with the kinetic and quantum yield data, which does not invoke $O_2^-$·, is presented in Scheme IV.

**Acknowledgment.** This work was supported by grants from the National Science Foundation and the National Institutes of Health.

## References and Notes

(1) R. Maskiewicz, D. Sogah, and T. C. Bruice, *J. Am. Chem. Soc.*, preceding paper in this issue.
(2) (a) J. R. Totter, *Photochem. Photobiol.*, **3**, 231 (1964); (b) J. R. Totter and G. Philbrook, *ibid.*, **5**, 177 (1966); (c) J. R. Totter in "Bioluminescence in Progress", E. H. Johnson, J. W. Hastings, and Y. Haneda, Eds., Princeton University Press, Princeton, N.J., 1966, pp 23–33; (d) J. R. Totter, *Photochem. Photobiol.*, **22**, 203 (1975).
(3) (a) E. G. Janzen, J. B. Pickett, J. W. Happ, and W. DeAngelis, *J. Org. Chem.*, **35**, 88 (1970); (b) J. W. Happ and E. G. Janzen, *ibid.*, **35**, 96 (1970).
(4) (a) K. Maeda and T. Hayashi, *Bull. Chem. Soc. Jpn.*, **40**, 169 (1967); (b) K. Maeda, T. Kashiwabara, and M. Tokuyama, *ibid.*, **50**, 473 (1977).
(5) K. D. Legg and D. M. Hercules, *J. Am. Chem. Soc.*, **91**, 1902 (1969).
(6) E. Rapaport, M. W. Cass, and E. H. White, *J. Am. Chem. Soc.*, **94**, 3160 (1972).
(7) F. Krohnke and H. L. Honig, *Chem. Ber.*, **90**, 2226 (1957).
(8) K. Gleu and R. Schaarschmidt, *Chem. Ber.*, **73**, 909 (1940); H. Decker and W. Petsch, *J. Prakt. Chem.*, **143**, 211 (1939).
(9) A. M. Grigorovskii and A. A. Simeonov, *J. Gen. Chem. USSR (Engl. Transl.)*, **21**, 589 (1951).
(10) K. Lehmstedt and H. Hundertmark, *Chem. Ber.*, **62**, 1065 (1929).
(11) K. Lehmstedt and H. Hundertmark, *Chem. Ber.*, **64**, 2386 (1931); A. Pictet and E. Patry, *ibid.*, **35**, 2536 (1902).
(12) L. Greenlee, I. Fridovich, and P. Handler, *Biochemistry*, **1**, 779 (1962).
(13) P. Ballinger and F. Long, *J. Am. Chem. Soc.*, **81**, 1050 (1959).
(14) B. P. Straughan and S. Walker, Eds., "Spectroscopy", Vol. 1, Chapman and Hall, London, 1976, pp 219–221.

# Total Synthesis of (±)-Pederamide

**Michael A. Adams,[1] Angelina J. Duggan, Joel Smolanoff, and Jerrold Meinwald***

*Contribution from the Department of Chemistry, Cornell University, Ithaca, New York 14853.* *Received February 26, 1979*

**Abstract:** The synthesis of (±)-pederamide (**2**), a key intermediate in the projected total synthesis of pederin (**1a**), a vesicant component of the hemolymph of the staphylinid beetle *Paederus fuscipes*, is described. The preparation of **2** is accomplished in 16 steps, starting from *trans*-2-butene epoxide.

Pederin, **1a**, a vesicant component in the hemolymph of many species of staphylinid beetle (genus *Paederus*), is a powerful inhibitor of protein synthesis in eucaryotic cells.[2]

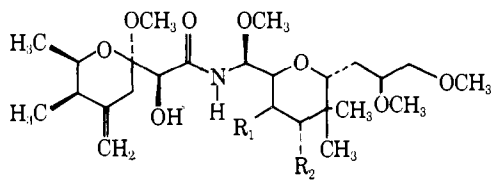

**1a**, $R_1$ = H; $R_2$ = OH
**b**, $R_1$ = OH; $R_2$ = H

Although the marked vesicatory effect of these beetles on man and animals was described as early as 1912,[3] it was not until 1949 that the principle responsible for this action was isolated by A. Ueta.[4] Pavan and Bo, in an independent study, obtained the active component contained in the hemolymph of *Paederus fuscipes* in crystalline form, and named it "pederin".[5]

Pederin was initially formulated as **1b**, based primarily on degradative studies.[6] Detailed NMR spectral analysis,[7] however, suggested that the structure was better represented as **1a**; this was confirmed by two independent X-ray crystallographic studies, carried out on the corresponding bis(*p*-bromobenzoate) of pederin. This work also established the absolute configuration of **1a**.[8]

Investigations of the acid-catalyzed hydrolysis of pederin have yielded, as the major products, pederamide (**2**), pederenal (**3**), and meropederin acetal (**4**), depending on the choice of

0002-7863/79/1501-5364$01.00/0 